SARDINIA RADIO TELESCOPE FINITE ELEMENT MODEL UPDATING BY MEANS OF PHOTOGRAMMETRIC MEASUREMENTS

FLAVIO STOCHINO, ANTONIO CAZZANI, SERGIO POPPI, AND EMILIO TURCO

Dedicated to Dr. R. A. Toupin in recognition of his outstanding contribution to Mechanics

Abstract. The 64-meter diameter Sardinia Radio Telescope (SRT), located near Cagliari (Italy), is the world's second largest fully steerable radio telescope with an active surface. Among its peculiarities there is the capability of modifying the configuration of the primary mirror surface by means of electro-mechanical actuators. This capability ensures, within a fixed range, the balancing of the deformation caused by external loads. In this way it can reduce the difference between the ideal shape of the mirror (which maximizes its performances) and the actual surface. The control-loop of the radio telescope needs a procedure which is able to predict SRT deformation, with the required accuracy, in order to reduce the deviation from the ideal shape. To achieve this aim a finite element (FE) model able to accurately predict the displacements of the structure is required. Unfortunately, the FE model of SRT, although very refined, does not give completely satisfactory results since it does not take into account essential pieces of information like, for instance, thermal strains and assembly defects. This paper explores a possible update of FE model using the only benchmark data available, *i.e.* the photogrammetric survey developed during the setup of the reflecting surface. This updating leads to a significant reduction of the differences between photogrammetric measurements and results of the numerical model. The effectiveness of this tuning procedure is thus assessed.

1. Introduction

Sardinia Radio Telescope, briefly SRT, is the world second largest fully steerable antenna with an active surface. An accurate description of SRT (see [1, 2]) goes beyond the aims of this paper and so only the most peculiar issues which are necessary to enhance the understanding of this work are highlighted.

Starting from the foundation and proceeding upward (see Figure 1 and Figure 2) it is possible to distinguish:

(1) the circular foundation ring on which the whole structure can completely rotate about the azimuthal axis along a circular rail;
(2) the alidade which connects the foundation ring to the elevation gear which is able to set the zenith axis of the antenna;
(3) the back up structure, connected to the elevation gear, which supports the primary mirror;
(4) the primary mirror, whose diameter is equal to 64 m, controlled, within a limited range, by means of 1104 electro-mechanical actuators acting on mirror panels for fine tuning, see Figure 3;

Date: April 20, 2021.

Key words and phrases. Sardinia Radio Telescope, Finite Element Model Updating, Structural Modelling, Huge Structures, Active Structures, Tikhonov's regularization, Generalized Cross Validation Criterion, Singular Value Decomposition.

(5) the quadrupod which supports the secondary mirror, according to a Gregorian configuration;
(6) the secondary mirror position can also be controlled, but only by means of rigid body motions.

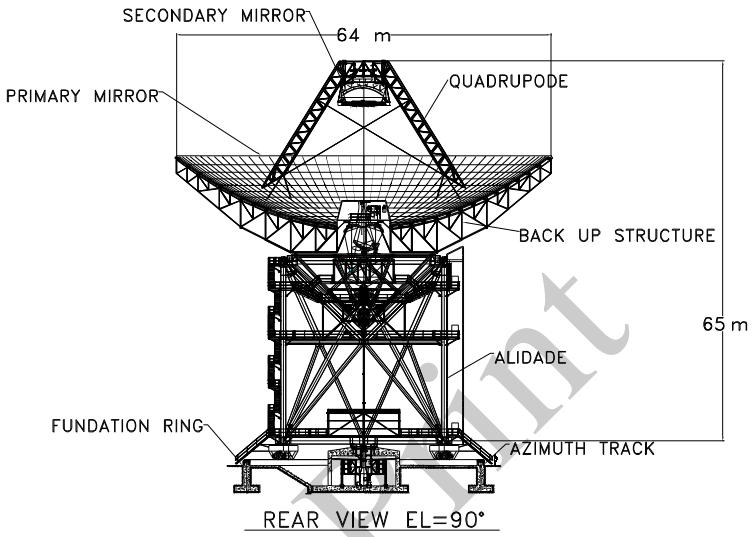

(a) Rear view at elevation $\beta = 90°$

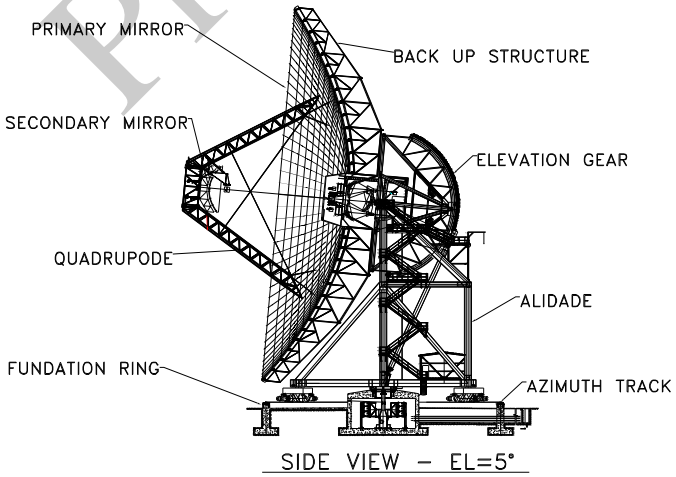

(b) Side view at elevation $\beta = 5°$

Figure 1. Sketch of SRT which highlights the main parts of the radio telescope.

Please cite this document as: F. Stochino, A. Cazzani, S. Poppi, and E. Turco "Sardinia Radio Telescope Finite Element Model Updating by means of Photogrammetric Measurements" Mathematics and Mechanics of Solids, Vol 22(4), 885–901 DOI:10.1177/1081286515616046

In order to perform accurate measurements SRT requires an extremely accurate configuration of the primary mirror's active surface. It is necessary to minimize the differences between the ideal and the real shapes; so a full recovery of the deformation caused by external loads like self-weight, temperature gradients, wind and so on is therefore required.

To clarify what is meant by extremely accurate configuration it is necessary to say that SRT has been designed to operate in the frequency range between 300 MHz and 100 GHz. In rough terms, this means that the differences, measured for example by the root mean square (RMS) deviation, between the optimal configuration and the actual one has to be less than 0.15 mm (*i.e.* 150 μm), at the working frequency of 100 GHz to achieve an antenna efficiency of 67% in precision measurements [2].

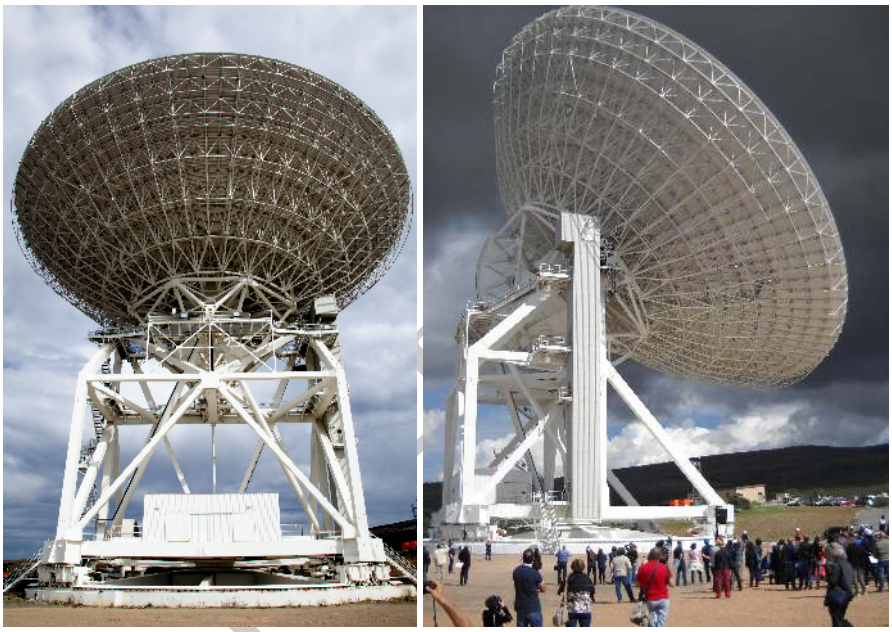

(a) $\beta = 90°$ (b) $\beta = 5°$

Figure 2. A view of the SRT at elevation angles 90° and 5°.

Nowadays the active surface configuration of SRT is regulated by means of some measurements based on photogrammetric techniques, which have been performed for elevation angles $\beta = 15°, 30°, 45°, 60°, 75°, 90°$, see [3].These measurements allow determining the elongation of each electro-mechanical actuator which is necessary to optimally configure the primary mirror. For elevation angles that are different from the above mentioned ones, actuators displacements are obtained by linear interpolation between the nearest known configurations.

On the other hand, it is clear that a very important radio telescope such as SRT has to be controlled accurately and in real time, if possible, in order to maximize its efficiency. In other words, starting from the requested configuration, azimuth and elevation angles, and from a series of environmental data, for example temperature and wind (even though in strong wind conditions SRT cannot work at maximum efficiency), a procedure which is able to predict the related displacements and suitable corrections by means of the electro-mechanical actuators is required.

Please cite this document as: F. Stochino, A. Cazzani, S. Poppi, and E. Turco "Sardinia Radio Telescope Finite Element Model Updating by means of Photogrammetric Measurements" Mathematics and Mechanics of Solids, Vol 22(4), 885–901 DOI:10.1177/1081286515616046

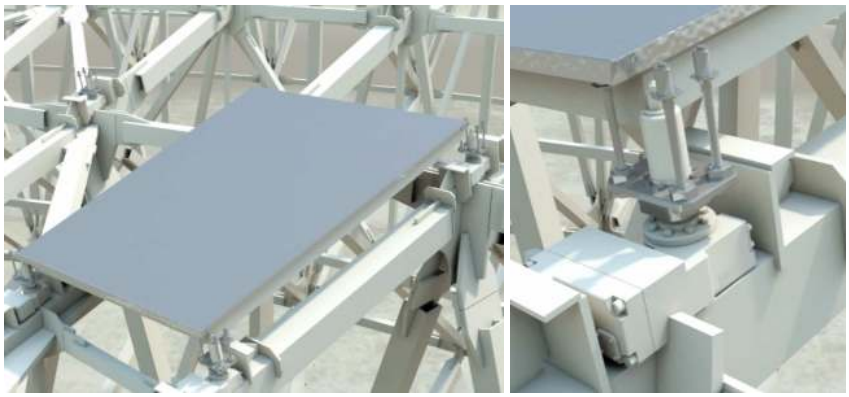

(a) Primary mirror panel on four actuators (b) Actuator detail

Figure 3. Electro-mechanical actuators.

A very refined finite element (FE) model of the radio telescope (composed by 93635 elements and 92788 nodes, corresponding to 463871 degrees-of-freedom) which has been used during the design phase is available.[1] This model, however, does not take into account all the effects, like construction faults and misalignments of the real members, thermal gradients and so on, which have a significant influence on the response of a statically undetermined structure such as SRT. As a consequence, numerical tests produce somewhat unsatisfactory results from the accuracy point of view and are not overall in-line with SRT requirements. In other words, displacements computed by means of SRT finite element model are somewhat different from those obtained by photogrammetric measurements.

In the authors' opinion, this depends on a lack of essential input data of the FE model. For example, no pieces of information about manufacturing flaws are present, thermal loads were not been taken into account, and so on. On the other hand, thermal effects have a strong influence on displacements and therefore on SRT primary mirror configuration which significantly reduce SRT performance. This is well documented, for example, in various papers [4, 5, 6, 7, 8, 9, 10, 11]. In addition FE models of radio telescopes are also available in the literature, see for example [12, 13]. As a consequence, the FE model has to be updated in order to adequately match the photogrammetric measurements which can be considered as a kind of experimental test on the actual SRT structure. There exists an extended bibliography on model updating: the authors mention here [14, 15, 16] for the main guidelines on methodology and [17, 18, 19, 20, 21, 22, 23, 24, 25] as examples of technical applications.

To the best of the authors' knowledge there are no other examples of the use of photogrammetric measurements to update finite element model of a large structure such as the SRT; indeed, in this case, the existence of these experimental data allows updating the FE model. However only the accuracy gain on astronomical measurements can be used as a decisive test to confirm the quality of results produced by the procedure which is proposed here. Indeed, the reduction of the actual reflecting surface RMS produces an improvement of the antenna gain which can be expressed by means of Ruze's equation: see [26].

[1]The first FE model was developed by BCV Progetti srl for the radio telescope structural design. The authors modified it taking into account all the differences between the designed structure and the actual one: for instance the lack of the thermic shield.

Please cite this document as: F. Stochino, A. Cazzani, S. Poppi, and E. Turco "Sardinia Radio Telescope Finite Element Model Updating by means of Photogrammetric Measurements" Mathematics and Mechanics of Solids, Vol 22(4), 885–901
DOI:10.1177/1081286515616046

The main goal of this work is to improve the finite element model (in particular its loads combination scheme), depicted in Figure 4, in order to make its results as close as possible to the actual structural response, in terms of displacements, using as feed back data those deriving from photogrammetry. To this end, in Section 2 the main points of the proposed strategy are sketched, while in Section 3 some numerical results showing the performance of the updated model are discussed. Finally, in Section 4 concluding remarks and future developments are outlined.

2. Finite Element Model Updating Procedure

By adopting the typical language of finite elements, the main guidelines to build a numerical model, which is able to accurately describe the SRT deformation is briefly sketched.

The ideal geometry of SRT, *i.e.* the optimal shape from the *optical* point of view, is known and can be assumed as a reference configuration for it. In a linear elasticity framework, a finite element model links the vector of nodal displacements $\mathbf{u}$ associated to a load vector $\mathbf{p}$ by means of a stiffness matrix $\mathbf{K}$ resulting in a linear system of simultaneous algebraic equations which enforces the equilibrium conditions:

$$\mathbf{K}\mathbf{u} = \mathbf{p}\,. \tag{1}$$

Different load conditions can be analyzed at once producing displacements relative to each one of them. For example, naming $\mathbf{p}_b$ and $\mathbf{p}_t$ those load vectors which are associated, respectively, to self-weight and to temperature increments with respect to the real shape assumed by SRT (which is only approximated by the FE model and is therefore unfortunately unknown), the corresponding displacements $\mathbf{u}_b$ and $\mathbf{u}_t$ can be easily calculated by solving the system of equations (1).

If one considers vector $\mathbf{e}_a$, which collects assigned anelastic strains, that represent strains that are not related to stresses (*i.e.* deriving from temperature increments or from manufacture flaw), the equivalent nodal load $\mathbf{p}_a$ can be computed as:

$$\mathbf{p}_a = \mathbf{D}^T\mathbf{C}\mathbf{e}_a\,, \tag{2}$$

if $\mathbf{D}^T$ and $\mathbf{C}$ are the equilibrium and the elastic compliance matrices respectively.

Displacement vector related to this last load vector can be formally evaluated as:

$$\mathbf{u}_a = \mathbf{K}^{-1}\mathbf{D}^T\mathbf{C}\mathbf{e}_a\,. \tag{3}$$

Matrix $\mathbf{A} := \mathbf{K}^{-1}\mathbf{D}^T\mathbf{C}$ is usually called the influence matrix and links anelastic strains vector and nodal displacements vector of the structural model. It can be noticed that, in general, the influence matrix is not square.

For some fixed configuration of SRT, namely those corresponding to elevation angles β equal to $\{15°, 30°, 45°, 60°, 75°, 90°\}$, displacements, were estimated by means of photogrammetric measurements and therefore are available, see [3].[2]

Thus, displacements can be treated as experimental data and represent the right hand side of Equation (3) while vector $\mathbf{e}_a$ is, in this problem, the unknown vector. Photogrammetric measurements of displacements surely contain self-weight contributions (*i.e.* a special case of body forces) while no information on temperature influence or on flaws/stretchings due to assembly can be deduced. Photogrammetic surveys were developed at night-time

[2]Even if there are other modern techniques of measurements, which are more accurate in some cases, only photogrammetric measurements are currently available. Furthermore, this paper sketches a procedure which can be easily adapted to other kinds of measurements.

Please cite this document as: F. Stochino, A. Cazzani, S. Poppi, and E. Turco "Sardinia Radio Telescope Finite Element Model Updating by means of Photogrammetric Measurements" Mathematics and Mechanics of Solids, Vol 22(4), 885–901
DOI:10.1177/1081286515616046

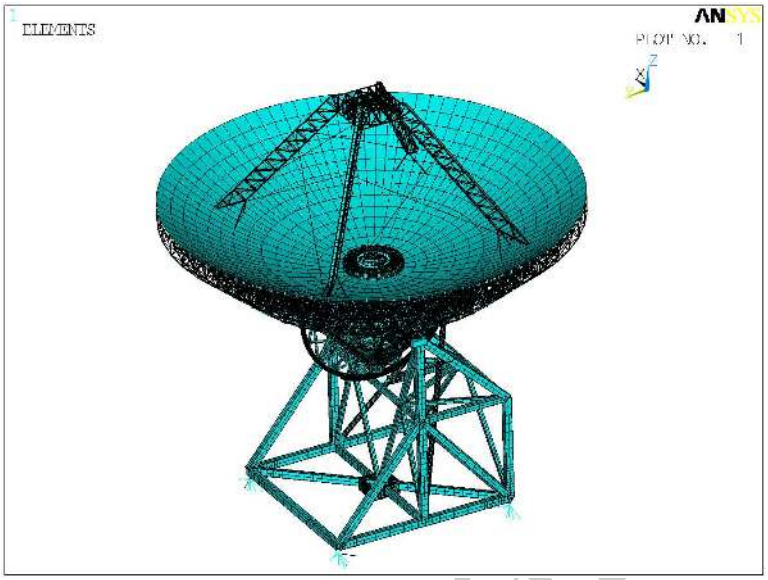

Figure 4. The FE model of SRT at an elevation angle of 90°.

(to avoid the influence of temperature gradients due to sun radiation) in two consecutive days, under environmental temperature approximately constant and equal to 22°C.

If we denote by $\mathbf{u}$ the total measured displacements, obtained in this case by photogrammetric survey, we can write

$$\mathbf{u} = \mathbf{u}_b + \mathbf{u}_a + \mathbf{u}_n \,, \tag{4}$$

where, in addition to the already defined vectors $\mathbf{u}_b$, $\mathbf{u}_a$, vector $\mathbf{u}_n$ takes care of the noise produced, for example, by errors on photogrammetric measurements, mechanical modeling assumptions and numerical approximations. Solving the system of equations:

$$\mathbf{A}\mathbf{e}_a = \mathbf{u} - \mathbf{u}_b - \mathbf{u}_n := \bar{\mathbf{u}} \,, \tag{5}$$

gives the anelastic strains which better describes the observed data.

The overdetermined linear algebraic system of equations (5) deserves some remarks:

(1) its coefficient matrix is rectangular and, in general, has (or should have) more rows than columns[3];
(2) it is ill-conditioned since, in rough terms, it tries to estimate displacements by strains, see for example [27, 28, 29, 30];
(3) its right hand side is surely affected by errors, as it has been mentioned above.

For these reasons an *ad hoc* solution strategy, which takes into account the specific peculiarities of the problem, has to be built. Singular Value Decomposition, briefly SVD, of the influence matrix $\mathbf{A}$ is useful to single out its main characteristics, see [31] and [32] for details. In formula, we can write this decomposition as

$$\mathbf{A} = \mathbf{W}\mathbf{\Sigma}\mathbf{V}^{\mathrm{T}} = \sum_{i=1}^{n} \mathbf{w}_i \sigma_i \mathbf{v}_i^{\mathrm{T}} \,, \tag{6}$$

[3]This means that the number of conditions to satisfy is larger than available unknowns.

Please cite this document as: F. Stochino, A. Cazzani, S. Poppi, and E. Turco "Sardinia Radio Telescope Finite Element Model Updating by means of Photogrammetric Measurements" Mathematics and Mechanics of Solids, Vol 22(4), 885–901 DOI:10.1177/1081286515616046

where matrices $\mathbf{W}$ and $\mathbf{V}$, whose dimensions are respectively $m \times m$ and $n \times n$, and whose columns are the orthonormal vectors $\mathbf{w}_i$ and $\mathbf{v}_i$, *i.e.* the left and right singular vectors. Instead $\mathbf{\Sigma}$ is a generalized diagonal matrix, whose dimensions are $m \times n$ and which have nonnegative diagonal terms equal to σ_i, the singular values of $\mathbf{A}$, see [31] for further details. By using this approach, the degree of ill-conditioning of matrix $\mathbf{A}$ is easy to compute, being simply the ratio between the maximum and the minimum singular values, *i.e.* the condition number. Moreover, SVD furnishes a simple representation of the solution of system (5):

$$\mathbf{e}_a = \sum_{i=1}^{n} \frac{\mathbf{w}_i^{\mathrm{T}} \bar{\mathbf{u}}}{\sigma_i} \mathbf{v}_i \,. \tag{7}$$

Equation (7), besides providing explicitly the solution, highlights the main difficulty in solving ill-conditioned discrete problems. The presence of very small singular values at the denominator of equation (7) surely amplify $\mathbf{w}_i^{\mathrm{T}} \bar{\mathbf{u}}$ and, therefore, also the errors which are inavoidably contained in the right hand side term $\bar{\mathbf{u}}$.

For an effective solution of (5), which is an ill-conditioned system of equations and at the same time contains in the r.h.s. errors that need to be filtered, the so-called Tikhonov approach [33] is very effective. Indeed, starting from a least square formulation of system (5)

$$\min \left\{ \|\mathbf{A}\mathbf{e}_a - \bar{\mathbf{u}}\|^2 \right\}, \tag{8}$$

a penalty term may be added, to constrain the solution with some a priori assumptions, by means of a Lagrangean multliplier λ, also known as a *regularization parameter*, which weighs a regularization term:

$$\min \left\{ \|\mathbf{A}\mathbf{e}_a - \bar{\mathbf{u}}\|_P^2 + \lambda^2 \|\mathbf{e}_a - \mathbf{e}_{a0}\|_Q^2 \right\} . \tag{9}$$

In equation (9), which has a somehow general form, $\mathbf{e}_{a0}$ is an estimate of the solution while the weighted norms, which are written here in a compact form as: $\|\mathbf{a}\|_P^2$ and $\|\mathbf{a}\|_Q^2$, are respectively defined as $\mathbf{a}^{\mathrm{T}}\mathbf{P}\mathbf{a}$ and $\mathbf{a}^{\mathrm{T}}\mathbf{Q}\mathbf{a}$. $\mathbf{P}$ and $\mathbf{Q}$ are two suitably defined square matrices: frequently, both of them are assumed to coincide with the identity matrix, while if no information about the solution is available, $\mathbf{e}_{a0}$ is chosen as a null vector. With these assumptions, the solution of equation (9) by using SVD is given by:

$$\mathbf{e}_a = \sum_{i=1}^{n} \sigma_i \frac{\mathbf{w}_i^{\mathrm{T}} \bar{\mathbf{u}}}{\sigma_i^2 + \lambda^2} \mathbf{v}_i \,, \tag{10}$$

which coincide with equation (7) when the value of the regularization parameter λ is equal to zero.

At this step the value of the regularizing parameter λ must be chosen. It controls how the constraint on the system of equation must be enforced in the solution. Technical bibliography contains many criteria to efficiently choose the regularization parameter λ, see for example [34]. However, in the authors opinion, one of the most interesting and widely used is a generalization of the Cross Validation Criterion proposed in [35] and extensively tested in [36, 37]. Its most attractive feature is that it does not require any information about the magnitude of error affecting the r.h.s. of the system of equations nor about how the error is distributed. Furthermore, as it will be shown later, its coding is very simple, particularly if SVD has been already computed. Only some insight are given here; interested readers can find additional cues about this topic in the original paper [35].

Denoting by $\mathbf{e}_{aj}(\lambda)$ the solution of equation (9) for an assigned value of λ, when the j-th equation is deleted, the corresponding residual of this regularized solution can be written

Please cite this document as: F. Stochino, A. Cazzani, S. Poppi, and E. Turco "Sardinia Radio Telescope Finite Element Model Updating by means of Photogrammetric Measurements" Mathematics and Mechanics of Solids, Vol 22(4), 885–901 DOI:10.1177/1081286515616046

as

$$\left\|\mathbf{A}\mathbf{e}_{aj}(\lambda) - \bar{\mathbf{u}}\right\|^2 = \left\|\mathbf{R}_j\left(\mathbf{A}\mathbf{e}_{aj}(\lambda) - \bar{\mathbf{u}}\right)\right\|^2 + \left(\mathbf{A}_j^{\mathrm{T}}\mathbf{e}_{aj}(\lambda) - \bar{\mathbf{u}}_j\right)^2 , \tag{11}$$

being $\mathbf{R}_j$ the operator which deletes the j-th row of matrix $\mathbf{A}$, while $\mathbf{A}_j$ is this deleted row. The two terms on the right hand side of equation (11) represent, respectively, the residual of the system of equations without the j-th row and the residual of the j-th row. Following the Cross Validation Criterion, the optimal value of the regularization parameter λ should not be related to a single observation. Therefore, equation (11) suggests to choose the value of λ coming out from

$$\min\left\{C(\lambda) := \sum_{j=1}^{m} g_j(\mathbf{A}_j^{\mathrm{T}}\mathbf{e}_{aj}[\lambda] - \bar{\mathbf{u}}_j)^2\right\}, \tag{12}$$

where g_j are the assumed weights for each observation, which give a measure of its reliability.

Cross Validation Criterion was generalized by using an additional condition for the weights g_j. This condition, that is quite reasonable, states that the optimal value of λ must be invariant with respect to any rotation of the coordinate system used for the measurements. This generalization, known as the Generalized Cross Validation Criterion, selects the optimal value of the regularization parameter λ by solving:

$$\min\left\{G(\lambda) := \frac{\mathbf{r}_\lambda^{\mathrm{T}}\mathbf{r}_\lambda}{\left(\mathrm{tr}\left(\mathbf{I} - \hat{\mathbf{A}}\right)\right)^2}\right\}, \tag{13}$$

where $\mathbf{r}_\lambda$ is the residual for an assigned value of λ and tr$(\cdot)$ indicates the trace operator. Formally, the resulting matrix $\hat{\mathbf{A}}$ is defined as

$$\hat{\mathbf{A}} = \mathbf{A}\left(\mathbf{A}^{\mathrm{T}}\mathbf{A} + \lambda^2\mathbf{I}\right)^{-1}\mathbf{A}^{\mathrm{T}} . \tag{14}$$

However, when the singular values σ_i of matrix $\mathbf{A}$ have been already computed, a simple way to evaluate the denominator of equation (13) is reported in [35] and gives:

$$\left(\mathrm{tr}\left(\mathbf{I} - \hat{\mathbf{A}}\right)\right)^2 = m - n + \sum_{i=1}^{n}\left(\frac{\lambda^2}{\lambda^2 + \sigma_i^2}\right), \tag{15}$$

where m and n denote, as already stated before, the dimensions of matrices $\mathbf{W}$ and $\mathbf{V}$.

It is crucial to point out that although the Generalized Cross Validation criterion is based on the assumption of Gaussian error distribution it works well, even if it is less accurate, also for errors which follow other distributions, [35].

The above sketched strategy is used to evaluate the anelastic strains $\mathbf{e}_a$, which need to be applied to the FE model in order to produce displacements as close as possible to those recorded by photogrammetric measurements (which here accept as an estimation of the actual one), once the effects of self weight have been depurated. In this sense, the finite element model is updated when anelastic strains $\mathbf{e}_a$ are known. It is essential to understand that these *equivalent* anelastic strains compensate the lack of information concerning two issues:

- all construction flaws, and the relative induced self-stresses, which make the actual structure to behave differently from the ideal one;
- a global estimate of deformations due to thermal effects, which are hardly predictable, since reference temperatures values at the construction time of each structural element are missing.

Please cite this document as: F. Stochino, A. Cazzani, S. Poppi, and E. Turco "Sardinia Radio Telescope Finite Element Model Updating by means of Photogrammetric Measurements" Mathematics and Mechanics of Solids, Vol 22(4), 885–901 DOI:10.1177/1081286515616046

After describing the updating procedure for the finite element model, some specific remarks on the SRT are listed in the following.

(1) Raw data deriving from photogrammetric measurements (PGM) are different from those computed by finite element code, since they are given in two different reference systems. Furthermore, photogrammetric data are manipulated to obtain actuator elongations which better reconstruct the optimal surface of primary mirror. However, before producing this fine tuning, a first correction is performed by means of a rigid motion of the secondary mirror.
(2) Each actuator, by means of its elongation, controls, at the same times, the configuration of two or four mirror panels: therefore optimal configuration is achieved only in an overall sense, and not at a completely local level.
(3) The influence matrix **A**, see equation (3), has been built considering only macro-element families (and not single elements). This choice resulted from an optimization process between the conflicting needs of achieving high accuracy while retaining a reasonable computational burden for the numerical model.

3. Numerical Results

In order to apply the above mentioned procedure to the FE model of the SRT, its principal mirror back up structure (see Figure 1) has been decomposed in simpler substructures. This is the only FE model part which has been considered for the updating procedure.

This choice is due to two reasons: first because of the back up structure static redundancy which makes it susceptible to thermal and self-stresses effects. Furthermore because the data, obtained by photogrammetric measurements, are referred only to the principal reflector points and the back up structure deformations have a paramount influence on the displacements of the primary mirror surface. It should be noticed that panels forming the reflecting surface have no structural role and therefore have not been included in the updating procedure.

Deformations of the alidade and of the secondary mirror mainly influence the pointing and focusing errors, but not the shape of the principal reflector, and can be easily compensated by a rigid body motion of the secondary mirror.

Therefore, 96 radial trusses, 15 hoop trusses and a central hub ring have been identified, as Figure 5 shows, and have been considered subjected to independent uniform anelastic strains of a yet unknown magnitude. To take advantage of the FE code these anelastic strains are assigned by a suitable distribution of differential temperatures. Indeed, once multiplied by the linear thermal expansion coefficient α of the constituent material (the SRT structure is made of steel characterized by $\alpha = 1.17 \times 10^{-5}\ ^{\circ}\mathrm{C}^{-1}$), they produce the required strains.

It is assumed that each substructures of these is subjected to an anelastic strain $\mathbf{e}_{as}$. Therefore all structural members belonging to the same substructures experience the same, uniform uniaxial anelastic strain. As a consequence, in this case the structure of matrix **A** consists of 1104 rows and 111 columns. The number of rows is equal to the number of the independent actuators of the principal mirror and the number of columns corresponds to that of chosen substructures.

As a measure of the global difference between the measured data, via photogrammetric measurements, and predictions of the finite element model the Root-Mean Square Deviation (RMSD) d, which can be defined as follows, has been selected:

$$d = \frac{\|\mathbf{r}\|}{\sqrt{n}}, \tag{16}$$

Please cite this document as: F. Stochino, A. Cazzani, S. Poppi, and E. Turco "Sardinia Radio Telescope Finite Element Model Updating by means of Photogrammetric Measurements" Mathematics and Mechanics of Solids, Vol 22(4), 885–901 DOI:10.1177/1081286515616046

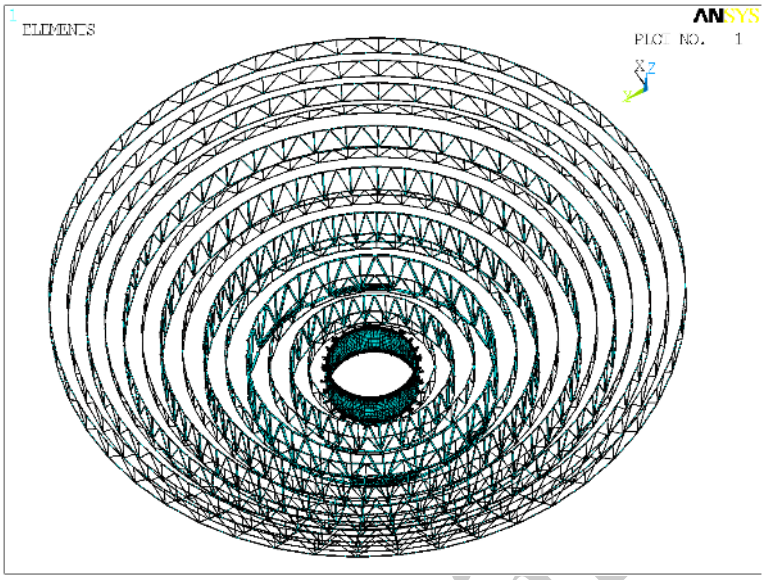

(a) The chosen 14 hoop trusses and the central hub ring.

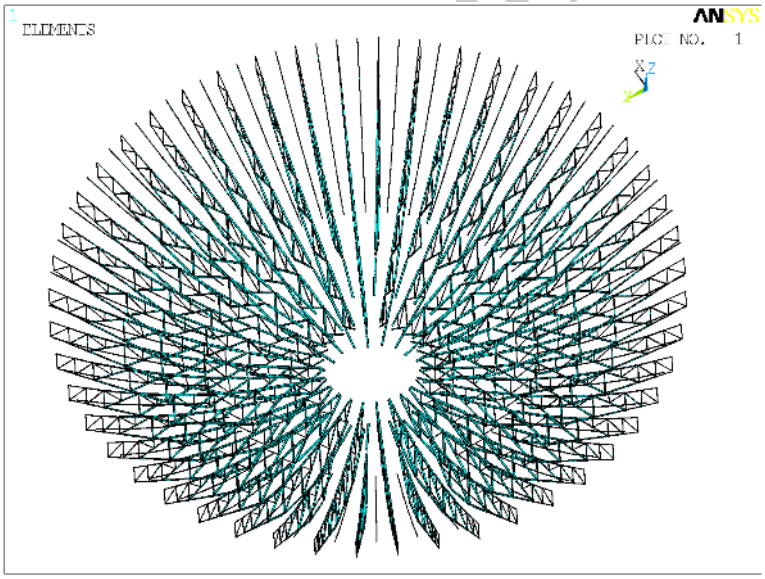

(b) The chosen 96 radial trusses.

FIGURE 5. Adopted sub structuring of the back up structure.

where $\|\mathbf{r}\|$ is the Euclidean norm of the difference between the displacements predicted via FE, $\mathbf{u}_b + \mathbf{A}\mathbf{e}_a$, and those measured and n the number of measurements, equal to 1104 in this case.

Using the procedure depicted in Section 2 a series of identification problems corresponding to the elevations β where photogrammetric data are taken has been solved. The values of the identified anelastic strains are depicted in Figures 6, 7, 8 and 9 for the four

Please cite this document as: F. Stochino, A. Cazzani, S. Poppi, and E. Turco "Sardinia Radio Telescope Finite Element Model Updating by means of Photogrammetric Measurements" Mathematics and Mechanics of Solids, Vol 22(4), 885–901 DOI:10.1177/1081286515616046

configurations considered and for each substructure. The shown values refer to equivalent differential temperatures. The actual anelastic strains can be computed by multiplying these values by the thermal linear expansion coefficient, α.

It is important to highlight that the geometrical symmetry doesn't correspond to a symmetric anelastic strain distribution; this confirms the presence of the above mentioned construction flaws and relative self induced stresses.

Figure 10 reports the corresponding plots of Generalized Cross Validation function, presented in equation (13), and its minimal value for the above mentioned elevation angles of the SRT. It is worth noticing that since the corresponding linear systems of equations are different the function graphs are different too. It is clear that an optimal solution is obtained for an elevation angle $\beta = 60°$: indeed, in this case we have a minimum d equal to 0.31476 mm and also the GCV function shows an absolute minimum value in this case, see Figure 10(b). Its value is below 10^{-4}, while in the other cases this function generally assumes higher values.

In order to present a summary form of the results obtained with the FE model and those with the updated FE model, in Table 1 the root mean square deviation, respect to photogrammetric measurements, of FE model (d_{FEM}) and updated FE model (d_{UpFEM}) belong with the percentage gain are reported. There is a significant improvement of the performance for each elevation angle and the relative maximum is obtained for the 75° elevation angle. In this case there is a FE model performance enhancement equal to the 43% with a value of d_{UpFEM} which has a magnitude of four hundred of microns, which is very close to the SRT required accuracy. The minimum d_{UpFEM} is achieved for the configuration corresponding to the 60° elevation angle and it is equal to 0.31476 mm. The lowest percentage gain, 28%, corresponds to the 15° elevation angle. The results of this comparison are also depicted in Figures 11, 12, 13 and 14: the local differences between PGM and FEM before and after the updating for the four analyzed cases are represented with a chromatic scale which is kept fixed for any elevation.

Table 1. Root mean square deviation d values (in mm) and gain (in %) of the update model varying the elevation angle β.

β	d_{FEM}	d_{UpFEM}	Gain %
15°	0.50676	0.36379	28
60°	0.49074	0.31476	36
75°	0.72243	0.41005	43
90°	0.81382	0.50205	38

In order to evaluate how the updating procedure changed the results of the FE model the displacements in the direction of the azimuthal axis (which is also the global z-axis of the FE model reference system) with and without the updating are plotted in Figures 15, 16, 17 and 18. To improve readability, only the main mirror and the quadrupode are shown for the four analyzed cases and it can be noticed that the global distribution is not modified for each case in a qualitative way, even though there are some quantitative differences when minima or maxima are considered.

4. Concluding Remarks

The Sardinia Radio Telescope is a huge fully steerable radio telescope with an active surface. Its capability of modifying the configuration of the primary mirror surface by

Please cite this document as: F. Stochino, A. Cazzani, S. Poppi, and E. Turco "Sardinia Radio Telescope Finite Element Model Updating by means of Photogrammetric Measurements" Mathematics and Mechanics of Solids, Vol 22(4), 885–901
DOI:10.1177/1081286515616046

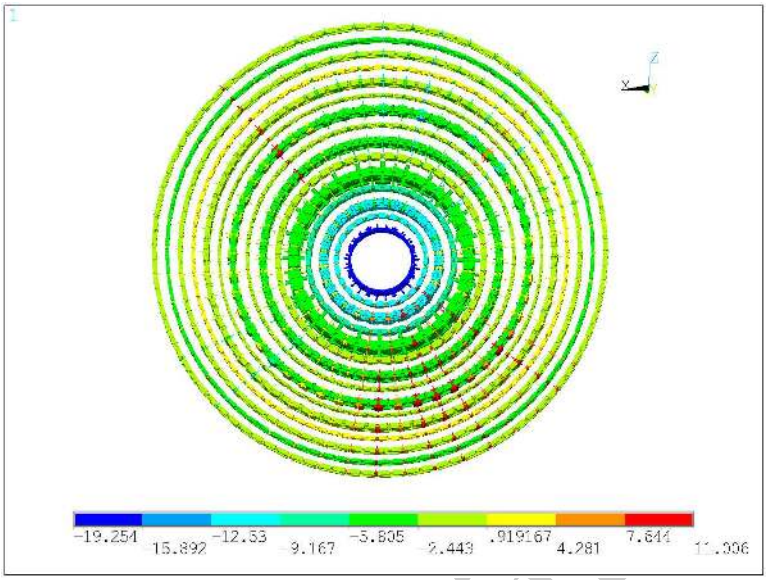

(a) Hoop trusses

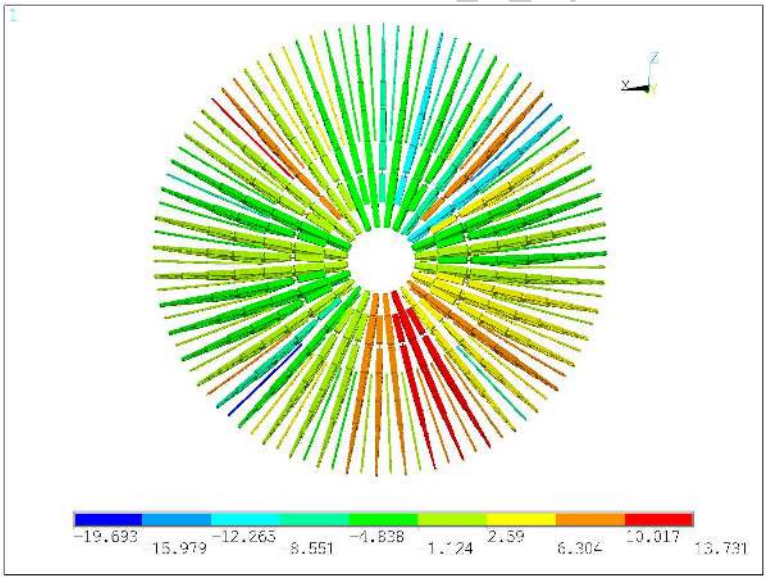

(b) Radial trusses

Figure 6. Anelastic strains distribution on hoop and radial trusses for elevation angle $\beta = 15°$.

means of electro-mechanical actuators allows it to balance the deformation caused by external loads, but requires a thorough estimation of the structural behavior. In this paper an approach to improve the accuracy of the finite element model is presented. The comparison with photogrammetric field recordings have shown a significant improvement of the FE model which emphasizes the effectiveness of the tuning procedure.

Please cite this document as: F. Stochino, A. Cazzani, S. Poppi, and E. Turco "Sardinia Radio Telescope Finite Element Model Updating by means of Photogrammetric Measurements" Mathematics and Mechanics of Solids, Vol 22(4), 885–901 DOI:10.1177/1081286515616046

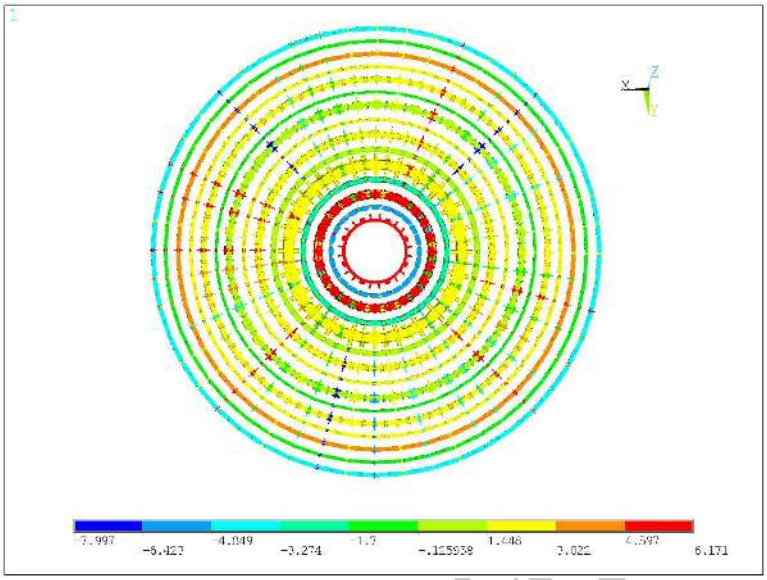

(a) Hoop trusses

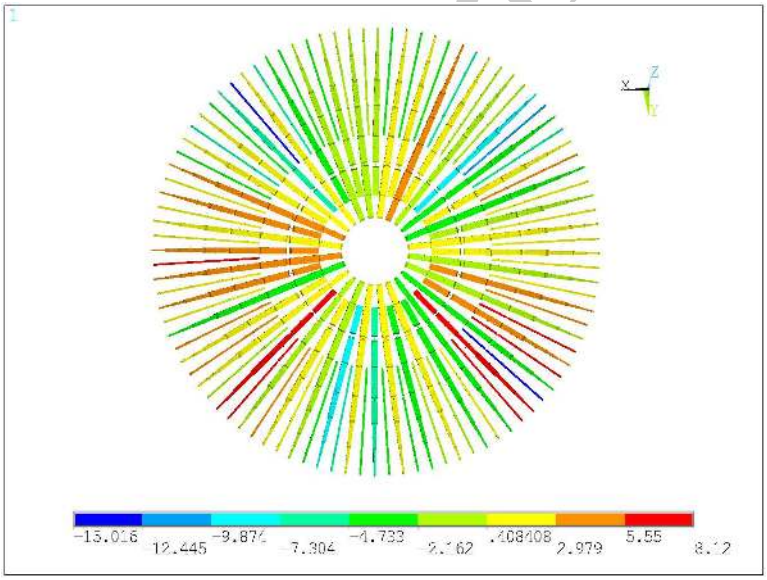

(b) Radial trusses

Figure 7. Anelastic strains distribution on hoop and radial trusses for elevation angle $\beta = 60°$.

The procedure described above, which globally takes into account, by means of anelastic strain distributions uniformly applied to groups of substructures, the deformations due to several causes (construction flaws, self induced stresses, etc.), whose effects are not and can not be estimated precisely enough, has proved a significant increase of the numerical model efficiency.

Please cite this document as: F. Stochino, A. Cazzani, S. Poppi, and E. Turco "Sardinia Radio Telescope Finite Element Model Updating by means of Photogrammetric Measurements" Mathematics and Mechanics of Solids, Vol 22(4), 885–901 DOI:10.1177/1081286515616046

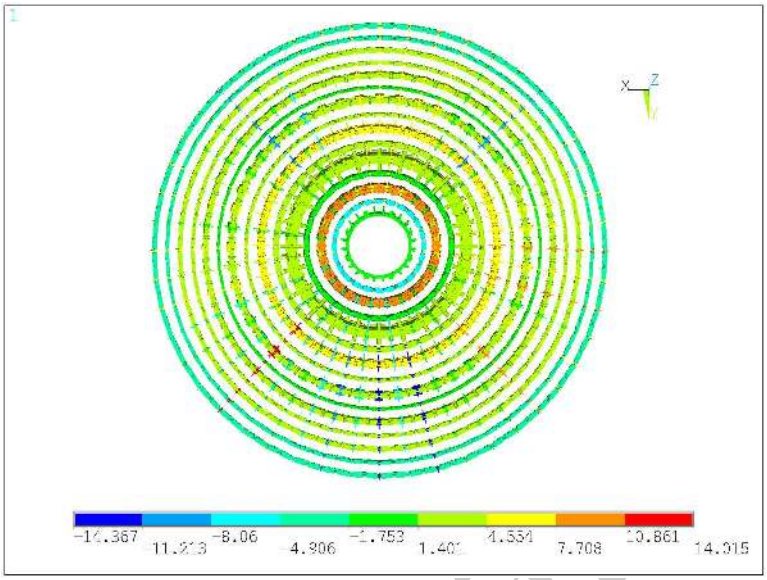

(a) Hoop trusses

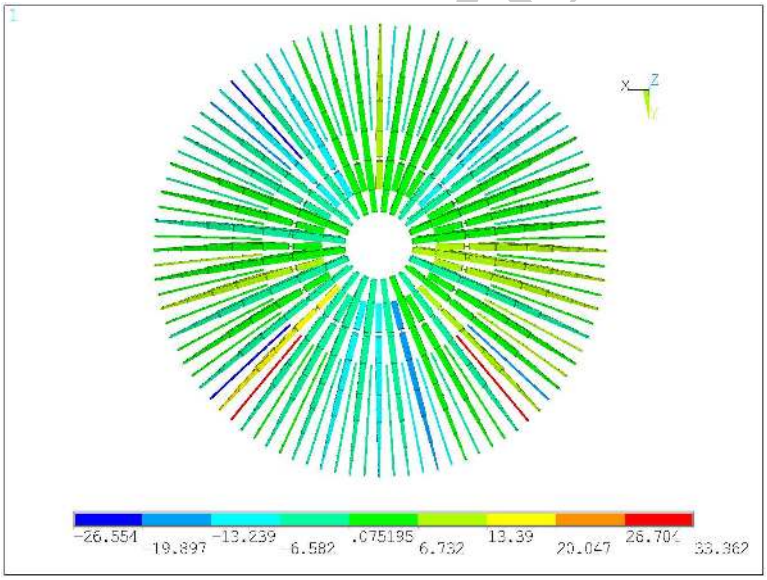

(b) Radial trusses

Figure 8. Anelastic strains distribution on hoop and radial trusses for elevation angle $\beta = 75°$.

In the present stage of the research these anelastic strains, whose determination is essential for computing the elongation of each actuator and which can be assimilated to the equivalent thermal strains produced by differential temperatures, turn out to be elevation-dependent. However, this is not acceptable from a physical point of view. To overcome this problem, the optimization process should be performed considering, on one hand, a

Please cite this document as: F. Stochino, A. Cazzani, S. Poppi, and E. Turco "Sardinia Radio Telescope Finite Element Model Updating by means of Photogrammetric Measurements" Mathematics and Mechanics of Solids, Vol 22(4), 885–901 DOI:10.1177/1081286515616046

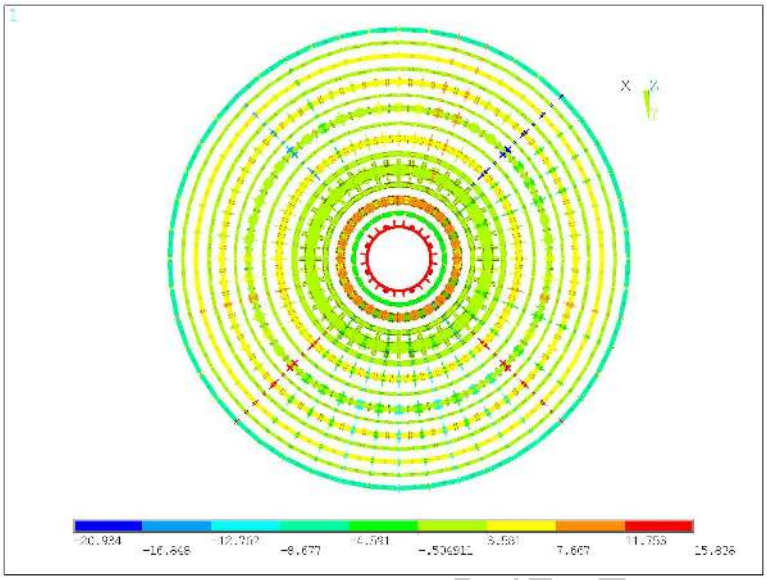

(a) Hoop trusses

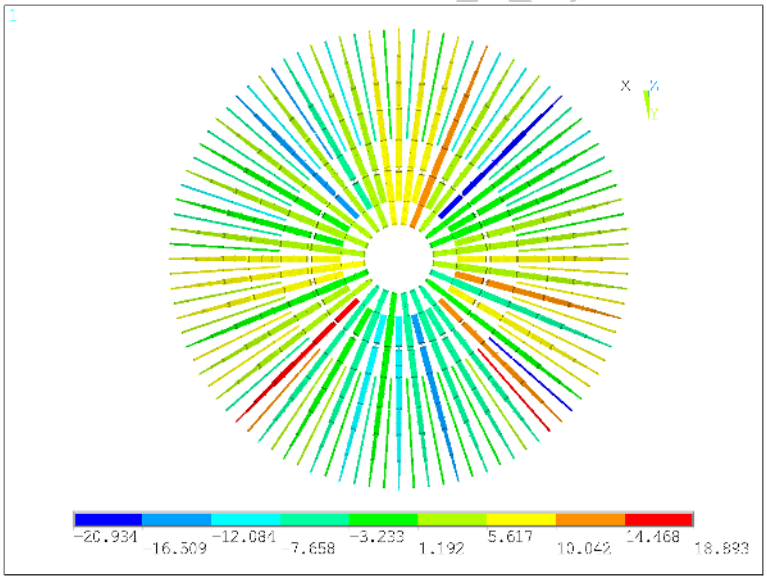

(b) Radial trusses

Figure 9. Anelastic strains distribution on hoop and radial trusses for elevation angle $\beta = 90°$.

larger number of variables (*i.e.* increasing the number of substructures considering that the maximum number is limited only by the available photogrammetric measurements and the required computational needs) and, on the other hand taking into account at the same time all available data (*i.e.* for all available elevations). In an intermediate step the elongation of each actuator could be computed interpolating the results for different elevation angles.

Please cite this document as: F. Stochino, A. Cazzani, S. Poppi, and E. Turco "Sardinia Radio Telescope Finite Element Model Updating by means of Photogrammetric Measurements" Mathematics and Mechanics of Solids, Vol 22(4), 885–901 DOI:10.1177/1081286515616046

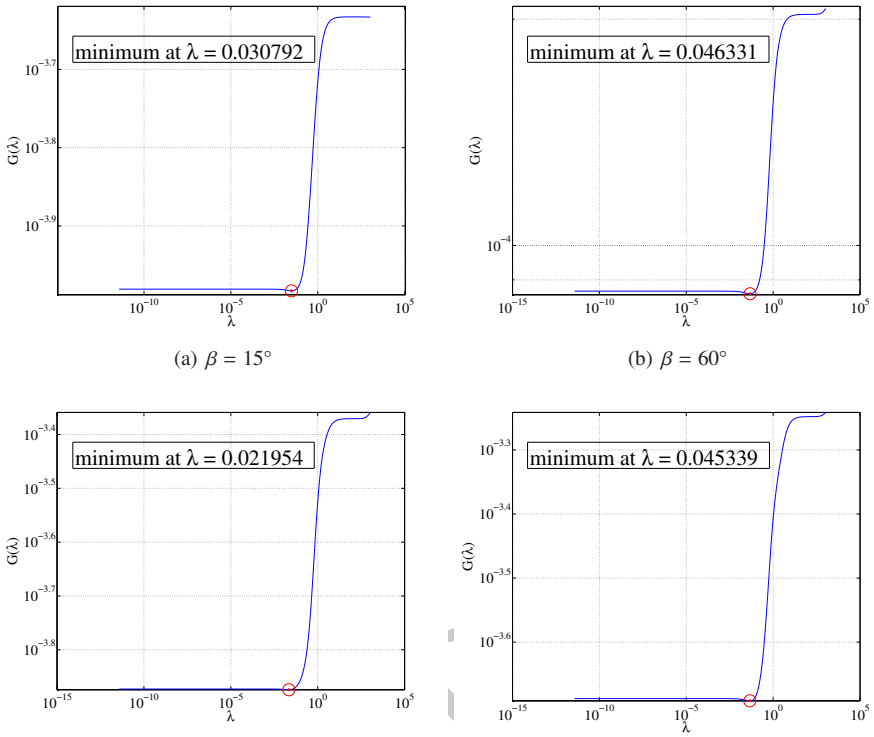

(a) $\beta = 15°$ (b) $\beta = 60°$

(c) $\beta = 75°$ (d) $\beta = 90°$

FIGURE 10. GCV function plots and the selected regularization parameter λ for several values of the elevation angle β.

Further developments are expected following this approach and also considering other field recordings of the SRT displacements coming from a set of holographic measurements which are currently being recorded, see [38]. In this way an enhanced FE model can be an effective part of the radio telescope control loop. In particular, if associated with real time information of climatic conditions (wind pressures, thermal load) recorded by sensors located on the main reflector surface, it will be able to thoroughly estimate on the fly the actuators elongations for any elevation angles.

In conclusion, this research line may produce useful results in classic and modern problems of mechanics, in particular in the framework of finite element model updating. Below there is a list of possible related fields and applications:

- refined numerical models, for example like those presented in [39, 40, 41] for beams or mixed and hybrid finite elements, see [42, 43, 44], which provide more accurate stress description also in the case of layered structures [45];
- buckling problems, like those described into [46, 47, 48, 49] and the papers cited therein, are very sensitive to stress level and so could benefit from its accurate evaluation;
- refined mathematical models are necessary to describe smart material; with this aim some authors use a suitable damage parameter, see [50, 51, 52, 53], paying

Please cite this document as: F. Stochino, A. Cazzani, S. Poppi, and E. Turco "Sardinia Radio Telescope Finite Element Model Updating by means of Photogrammetric Measurements" Mathematics and Mechanics of Solids, Vol 22(4), 885–901 DOI:10.1177/1081286515616046

particular attention to cases which leads to non-unique and non-stable solutions, see [54, 55, 56]; altenatively, there is the approach described in [57, 58] where a two-dimensional model for an interfacial zone is developed to describe concentrated damages; furthermore, it seems attractive the application of higher continuum models as those described in [59, 60, 61, 62];

- damage detection is an emerging and very important field which deserves attention; some examples are reported in [63, 64] which considers traveling loads as signal or in identification problem such as those described in [65, 66, 67, 68];
- extension to plasticity, with the aim to evaluate the collapse load, see for example [69, 70, 71, 72, 73, 74]; also the variational techniques presented in [75] is interesting for dissipative phenomena;
- smart materials such as those piezoelectric might be advantageously used to improve the structural control, see [76, 77].

Acknowledgement

The financial support of RAS, the Autonomous Region of Sardinia, under grant number CRP-26658 (L. R. 7/2007, year 2011 call, Project: *Deformation estimates of the Sardinia Radio Telescope*) is gratefully acknowledged.

References

[1] F. Buffa, A. Cazzani, A. Causin, S. Poppi, G. M. Sanna, M. Solci, F. Stochino, and E. Turco. The Sardinia Radio Telescope: a comparison between close range photogrammetry and FE models. *Mathematics and Mechanics of Solids*, submitted, 2015.

[2] T. Pisanu, F. Buffa, M. Morsiani, M. Natalini, C. Pernechele, and G. Vargiu. How to improve the high-frequency capabilities of the SRT. *Mem. S. A. It. Suppl.*, 10:136–140, 2006.

[3] M. Süss, D. Koch, and H. Paluszek. The Sardinia Radio Telescope (SRT) optical alignment. In *Ground–based and Airborne Telescopes IV. Proceedings of SPIEE*, number 84442G, pages 1–16, doi:10.1117/12.926141, 2012.

[4] K. I. Majid and S. P. Chiew. Design of radio telescope structural frameworks. *Engineering Structures*, 7:114–120, April 1985.

[5] A. Greve and M. Bremer. *Thermal Design and Thermal Behaviour of Radio Telescopes and their Enclosures*. Springer, 2010.

[6] R. B. Baraimov, I. V. Baum, M. A. Gurbanyazov, I. N. Knyazev, Y.I. Machuyev, and V. G. Fokin. *Climatic Influences on Antenna Systems*, volume (in Russian). Ashkhabad, 1988.

[7] Y. I. Machuyev and V. G. Gimmelman. Temperature state of radio antennas under climatic influences. In *7-th Int. Symp. on Antennas and EM Theory*, 2006.

[8] J. W. M. Baars, A. Greve, B. G. Hooghoudt, and J. Peñalver. Thermal control of the IRAM 30-m millimiter radio telescope. *Astronomy and Astrophysics*, 195:364–371, 1998.

[9] A. Greve and M. Bremer. Calculated thermal behavior of ventilated calculated thermal behavior of ventilated high precision radio telescopes. *IEEE Antennas and Propagation Magazine*, 48(3):9–19, 2006.

[10] J. W. Lamb and D. P. Woody. Thermal behavior of the Leighton 10-m antenna backing structure. *MMA Memo*, 234:1–11, 1998.

Please cite this document as: F. Stochino, A. Cazzani, S. Poppi, and E. Turco "Sardinia Radio Telescope Finite Element Model Updating by means of Photogrammetric Measurements" Mathematics and Mechanics of Solids, Vol 22(4), 885–901 DOI:10.1177/1081286515616046

[11] A. Greve, M. Bremer, J. Peñalver, P. Raffin, and D. Morris. Improvement of the IRAM 30-m telescope from temperature measurements and finite-element calculations. *IEEE Transactions on Antennas and Propagation*, 53(2):851–860, 2005.

[12] A. I. Borovkov, D. V. Shevchenko, A. V. Gaev, and A. S. Nemov. Finite element modeling and thermal analysis of the RT-70 radio telescope main reflector. In *Int. Conf. on Antenna Theory and Techniques*, pages 651–654, 2004.

[13] A. I. Borovkov, D. V. Shevchenko, A. V. Gaev, and A. S. Nemov. 3D finite element thermal and structural analysis of the RT-70 full-circle radio telescope. In *Proceedings of International ANSYS Conf*, 2004.

[14] M. I. Friswell and J. E. Mottershead. *Finite element model updating in structural dynamics*. Kluwer Academic Publisher, 1995.

[15] A. Aktan, N. Catbas, N. Türer, and Z. Zhang. Structural identification: analytical aspects. *Journal of Structural Engineering*, 124(7):817–829, 1998.

[16] A. De Sortis, E. Antonacci, and F. Vestroni. Dynamic identification of a masonry building using forced vibration tests. *Engineering Structures*, 27(2):155–165, 2005.

[17] M. Dilena and A. Morassi. Dynamic testing of damaged bridge. *Mechanical Systems and Signal Processing*, 25:1485–1507, 2011.

[18] M. Dilena, A. Morassi, and M. Perin. Dynamic identification of a reinforced concrete damaged bridge. *Mechanical Systems and Signal Processing*, 25:2990–3009, 2011.

[19] A. Morassi. Dynamic testing and structural identification of the Hypo Bank office complex. I: Experiments. *Journal of Structural Engineering ASCE*, 137(12):1527–1539, 2011.

[20] A. Morassi and F. Polentarutti. Dynamic testing and structural identification of the Hypo Bank office complex. II: Identification. *Journal of Structural Engineering ASCE*, 137(12):1540–1552, 2011.

[21] S. Bennati, L. Nardini, and W. Salvatore. Dynamic behavior of a medieval masonry bell tower. part I: Experimental measurements and modeling of bell's dynamic actions. *Journal of Structural Engineering*, 131(11):1647–1655, 2005.

[22] B. Moaveni and I. Behmanesh. Effects of changing ambient temperature on finite element model updating of the Dowling Hall Footbridge. *Engineering Structures*, 43:58–68, 2012.

[23] B. Richard, L. Adelaide, C. Cremona, and A. Orcesi. A methodology for robust updating of nonlinear structural models. *Engineering Structures*, 41(356–372), 2012.

[24] B. A. Zárate and J. M. Caicedo. Finite element model updating: Multiple alternatives. *Engineering Structures*, 30:3724–3730, 2008.

[25] H. Schlune, M. Plos, and K. Gylltoft. Improved bridge evaluation through finite element model updating using static and dynamic measurements. *Engineering Structures*, 31:1477–1485, 2009.

[26] J. Ruze. The effect of aperture errors on the antenna radiation pattern. *Nuevo Cimento Suppl*, 9(3):364–380, 1952.

[27] E. Turco. Load distribution modelling for pin-jointed trusses by an inverse approach. *Computer Methods in Applied Mechanics and Engineering*, 165:291–306, 1998.

[28] E. Turco. A boundary elements approach to identify static boundary conditions in elastic solids from stresses at internal points. *Inverse Problems in Engineering*, 7:309–333, 1999.

[29] E. Turco. Is the statistical approach suitable for identyfing actions on structures? *Computers and Structures*, 83:2112–2120, 2005.

Please cite this document as: F. Stochino, A. Cazzani, S. Poppi, and E. Turco "Sardinia Radio Telescope Finite Element Model Updating by means of Photogrammetric Measurements" Mathematics and Mechanics of Solids, Vol 22(4), 885–901 DOI:10.1177/1081286515616046

[30] E. Turco. Identification of axial forces on statically indeterminate pin–jointed trusses by a nondestructive mechanical test. *The Open Civil Engineering Journal*, 7:50–57, 2013.
[31] G. H. Golub and C. F. Van Loan. *Matrix computations*. The Johns Hopkins University Press, Baltimore and London, 3rd edition, 1996.
[32] S. Pellegrino. Structural computations with the singular value decomposition of the equilibrium matrix. *International Journal of Solids and Structures*, 30(21):3025–3035, 1993.
[33] A. N. Tikhonov and V. Y. Arsenin. *Solution of ill–posed problems*. John Wiley & Sons, New York, 1977.
[34] P. C. Hansen. Numerical tools for analysis and solution of Fredholm integral equations of the first kind. *Inverse Problems*, 8:849–872, 1992.
[35] G. H. Golub, M. Health, and G. Wahba. Generalized Cross–Validation as a method for choosing a good ridge parameter. *Technometrics*, 21(2):215–223, May 1979.
[36] A. Bilotta and E. Turco. A numerical study on the solution of the Cauchy problem in elasticity. *International Journal of Solids and Structures*, 46:4451–4477, 2009.
[37] E. Turco. An effective algorithm for reconstructing boundary conditions in elastic solids. *Computer Methods in Applied Mechanics and Engineering*, 190:3819–3829, 2001.
[38] G. Serra, P. Bolli, G. Busonera, T. Pisanu, S. Poppi, F. Gaudiomonte, G. Zacchiroli, J. Roda, M. Morsiani, and J. A. Lopez-Perez. Microwave holography system for the sardinia radio telescope. In *Proceedings of SPIEE*, pages 884:84445W–1–84445W–15, 2012.
[39] A. Cazzani, M. Malagù, and E. Turco. Isogeometric analysis of plane curved beams. *Mathematics and Mechanics of Solids*, published online 20 April 2014, DOI: 10.1177/1081286514531265:1–16, 2014.
[40] A. Cazzani, M. Malagù, F. Stochino, and E. Turco. Constitutive models for strongly curved beams in the frame of isogeometric analysis. *Mathematics and Mechanics of Solids*, (in print), 2014.
[41] Antonio Cazzani, Marcello Malagù, and Emilio Turco. Isogeometric analysis: a powerful numerical tool for the elastic analysis of historical masonry arches. *Continuum Mechanics and Thermodynamics*, published online 28 December 2014, DOI: 10.1007/s00161-014-0409-y:1–18, 2014.
[42] S. N. Atluri and A. Cazzani. Rotations in computational solid mechanics. *Archives of Computational Methods in Engineering*, 2:49–138, 1995.
[43] A. Cazzani and S. N. Atluri. Four–noded mixed finite elements, using unsymmetric stresses, for linear analysis of membranes. *Computational Mechanics*, 11:229–251, 1993.
[44] A. Cazzani and C. Lovadina. On some mixed finite element methods for plane membrane problems. *Computational Mechanics*, 20:560–572, 1997.
[45] A. Cazzani, E. Garusi, A. Tralli, and S. N. Atluri. A four–node hybrid assumed-strain finite element for laminated composite plates. *Computers, Materials & Continua*, 2:23–38, 2005.
[46] M. Pignataro and A. Luongo. Asymmetric interactive buckling of thin–walled columns with initial imperfections. *Thin–Walled Structures*, 5(5):365–382, 1987.
[47] A Luongo. Mode localization in dynamics and buckling of linear imperfect continuous structures. *Nonlinear Dynamics*, 25(1-3):133–156, 2001.

Please cite this document as: F. Stochino, A. Cazzani, S. Poppi, and E. Turco "Sardinia Radio Telescope Finite Element Model Updating by means of Photogrammetric Measurements" Mathematics and Mechanics of Solids, Vol 22(4), 885–901 DOI:10.1177/1081286515616046

[48] A. Luongo. On the amplitude modulation and localization phenomena in interactive buckling problems. *International Journal of Solids and Structures*, 27(15):1943–1954, 1991.

[49] M. Pignataro, A. Luongo, and N. Rizzi. On the effect of the local overall interaction on the postbuckling of uniformly compressed channels. *Thin–Walled Structures*, 3(4):293–321, 1985.

[50] A. Rinaldi and L. Placidi. A microscale second gradient approximation of the damage parameter of quasi–brittle heterogeneous lattices. *ZAMM - Zeitschrift für Angewandte Mathematik und Mechanik*, 1(16):DOI 10.1002/zamm.201300028, 2013.

[51] A. Rinaldi. A rational model for 2D disordered lattices under uniaxial loading. *International Journal of Damage Mechanics*, 18:233–257, 2009.

[52] A. Rinaldi. Statistical model with two order parameters for ductile and statistical model with two order parameters for ductile and soft fiber bundles in nanoscience and biomaterials. *Physical Review E (Statistical, Nonlinear, and Soft Matter Physics)*, 83(046126(10)), 2011.

[53] A. Madeo, L. Placidi, and G. Rosi. Towards the design of metamaterials with enhanced damage sensitivity: second gradient porous materials. *Research in Nondestructive Evaluation*, 25(2):99–124, 2014.

[54] V. A. Eremeyev and W. Pietraszkiewicz. The nonlinear theory of elastic shells with phase transitions. *Journal of Elasticity*, 74(1):67–86, 2004.

[55] V. A. Yeremeyev, A. B. Freidin, and L. L. Sharipova. The stability of the equilibrium of two-phase elastic solids. *Journal of Applied Mathematics and Mechanics*, 71(1):61–84, 2007.

[56] V. A. Eremeev, A. B. Freidin, and L. L. Sharipova. Nonuniqueness and stability in problems of equilibrium of elastic two–phase bodies. *Doklady Physics*, 48(7):359–363, 2003.

[57] F. dell'Isola and A. Romano. On the derivation of thermomechanical balance equations for continuous systems with a nonmaterial interface. *International Journal of Engineering Science*, 25(11-12):1459–1468, 1987.

[58] F. D'Annibale and A. Luongo. A damage constitutive model for sliding friction coupled to wear. *Continuum Mechanics and Thermodynamics*, 25(2-4):503–522, 2013.

[59] F. dell'Isola, P. Seppecher, and A. Madeo. How contact interactions may depend on the shape of cauchy cuts in n-th gradient continua: approach á la D'Alembert. *Zeitschrift für Angewandte Mathematik und Physik (ZAMP)*, 63(6):1119–1141, 2012.

[60] F. dell'Isola and P. Seppecher. The relationship between edge contact forces, double forces and interstitial working allowed by the principle of virtual power. *Comptes Rendus de l'Academie de Sciences - Serie IIb: Mecanique, Physique, Chimie, Astronomie*, 321:303–308, 1995.

[61] S. Federico, A. Grillo, S. Imatani, G. Giaquinta, and W. Herzog. An energetic approach to the analysis of anisotropic hyperelastic materials. *International Journal of Engineering Science*, 46:164–181, 2008.

[62] A. Misra. Mechanistic model for contact between rough surfaces. *Journal of Engineering mechanics*, 123(5):475–484, 1997.

[63] N. Roveri and A. Carcaterra. Damage detection in structures under travelling loads by the Hilbert–Huang transform. *Mechanical System and Signal Processing*, 28:128–144, 2012.

[64] M. Ferretti and G. Piccardo. Dynamic modeling of taut strings carrying a traveling mass. *Continuum Mechanics and Thermodynamics*, 25(2-4):469–488, 2013.

Please cite this document as: F. Stochino, A. Cazzani, S. Poppi, and E. Turco "Sardinia Radio Telescope Finite Element Model Updating by means of Photogrammetric Measurements" Mathematics and Mechanics of Solids, Vol 22(4), 885–901 DOI:10.1177/1081286515616046

[65] E. Turco. A strategy to identify exciting forces acting on structures. *International Journal for Numerical Methods in Engineering*, 64:1483–1508, 2005.
[66] G. Alessandrini, A. Bilotta, G. Formica, A. Morassi, E. Rosset, and E. Turco. Evaluating the volume of a hidden inclusion in an elastic body. *Journal of Computational and Applied Mathematics*, 198(2):288–306, 2007.
[67] G. Alessandrini, A. Bilotta, G. Formica, A. Morassi, E. Rosset, and E. Turco. Numerical size estimates of inclusions in elastic bodies. *Inverse Problems*, 21:133–151, 2005.
[68] G. Alessandrini, A. Bilotta, A. Morassi, and E. Turco. Computing volume bounds of inclusions by EIT measurements. *Journal of Scientific Computing*, 33(3):293–312, 2007.
[69] R. Contro, C. Poggi, and A. Cazzani. Numerical analysis of fire effects on beam structures. *Engineering Computations*, 5:53–58, 1988.
[70] A. Cazzani, R. Contro, and L. Corradi. On the evaluation of the shakedown boundary for temperature-dependent elastic properties. *European Journal of Mechanics A/Solids*, 11:539–550, 1992.
[71] U. Andreaus and P. Baragatti. Cracked beam identification by numerically analysing the nonlinear behaviour of the harmonically forced response. *Journal of Sound and Vibration*, 330(4):721–742, 2011.
[72] A. Cazzani and M. Rovati. Sensitivity analysis and optimum design of elastic-plastic structural systems. *Meccanica*, 26:173–178, 1991.
[73] E. Turco and P. Caracciolo. Elasto–plastic analysis of Kirchhoff plates by high simplicity finite elements. *Computer Methods in Applied Mechanics and Engineering*, 190:691–706, 2000.
[74] P. Neff, A. Sysow, and C. Wieners. Numerical approximation of incremental infinitesimal gradient plasticity. *International Journal for Numerical Methods in Engineering*, 77:414–436, 2009.
[75] F. dell'Isola, A. Madeo, and P. Seppecher. Boundary conditions at fluid–permeable interfaces in porous media: A variational approach. *International Journal of Solids and Structures*, 46(17):3150–3164, 2009.
[76] C. Maurini, J. Pouget, and F. dell'Isola. Extension of the Euler–Bernoulli model of piezoelectric laminates to include 3D effects via a mixed approach. *Computers and Structures*, 84:1438–1458, 2006.
[77] R. C. Batra, F. dell'Isola, S. Vidoli, and D. Vigilante. Multimode vibration suppression with passive two-terminal distributed network incorporating piezoceramic transducers. *International Journal of Solids and Structures*, 42:3115–3132, 2005.

DADU, Università degli Studi di Sassari, Asilo Sella, via Garibaldi 35, 07041 Alghero (SS), Italia.
Email address: fstochino@uniss.it

DICAAR, Università degli Studi di Cagliari, via Marengo 2, 09123 Cagliari (CA) Italia.
Email address: antonio.cazzani@unica.it

INAF–OAC Osservatorio Astronomico di Cagliari, via della Scienza 5, 09047 Selargius (CA) Italia.
Email address: spoppi@oa-cagliari.inaf.it

DADU, Università degli Studi di Sassari, Asilo Sella, via Garibaldi 35 07041 Alghero (SS), Italia.
Email address, Corresponding author: emilio.turco@uniss.it

Please cite this document as: F. Stochino, A. Cazzani, S. Poppi, and E. Turco "Sardinia Radio Telescope Finite Element Model Updating by means of Photogrammetric Measurements" Mathematics and Mechanics of Solids, Vol 22(4), 885–901 DOI:10.1177/1081286515616046

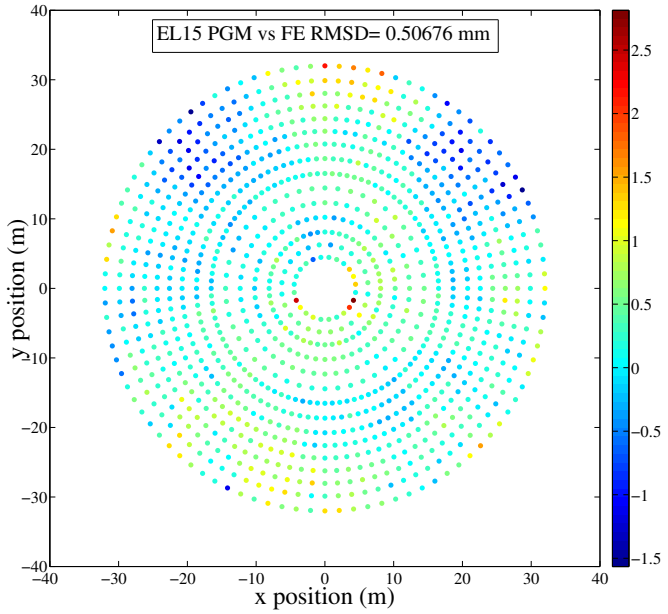

(a) Elevation $\beta = 15°$ without updating

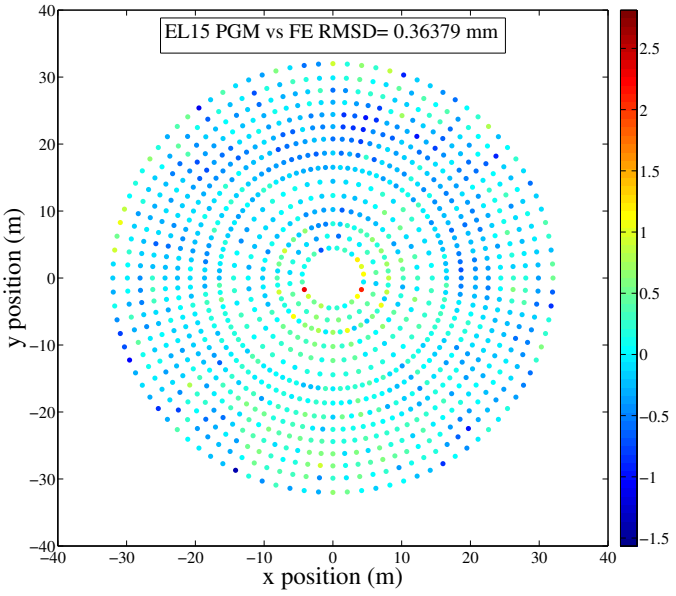

(b) Elevation $\beta = 15°$ with updating

Figure 11. FEM *vs* PGM comparison without (a) and with (b) model updating for elevation angle $\beta = 15°$. Chromatic scale of displacements is in mm.

Please cite this document as: F. Stochino, A. Cazzani, S. Poppi, and E. Turco "Sardinia Radio Telescope Finite Element Model Updating by means of Photogrammetric Measurements" Mathematics and Mechanics of Solids, Vol 22(4), 885–901 DOI:10.1177/1081286515616046

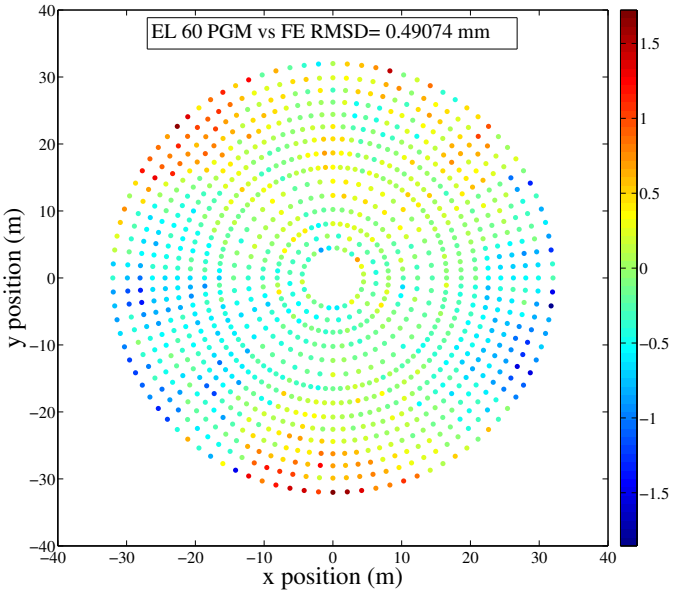

(a) Elevation $\beta = 60°$ without updating

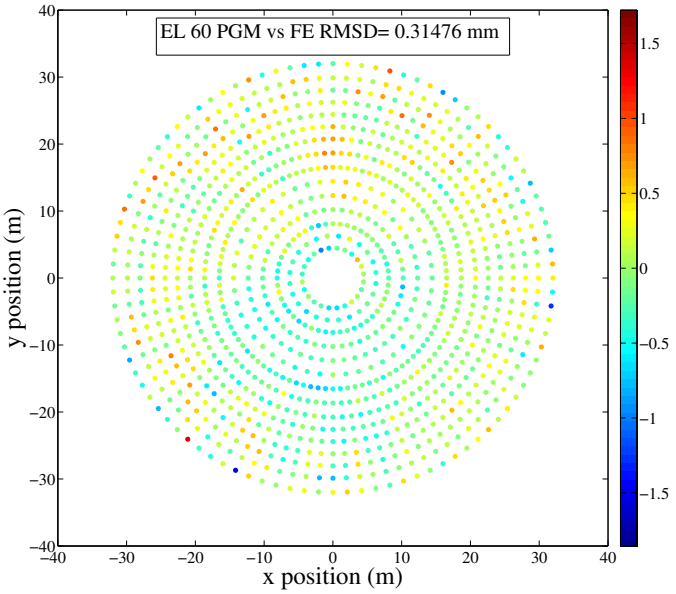

(b) Elevation $\beta = 60°$ with updating

Figure 12. FEM *vs* PGM comparison without (a) and with (b) model updating for elevation angle $\beta = 60°$. Chromatic scale of displacements is in mm.

Please cite this document as: F. Stochino, A. Cazzani, S. Poppi, and E. Turco "Sardinia Radio Telescope Finite Element Model Updating by means of Photogrammetric Measurements" Mathematics and Mechanics of Solids, Vol 22(4), 885–901 DOI:10.1177/1081286515616046

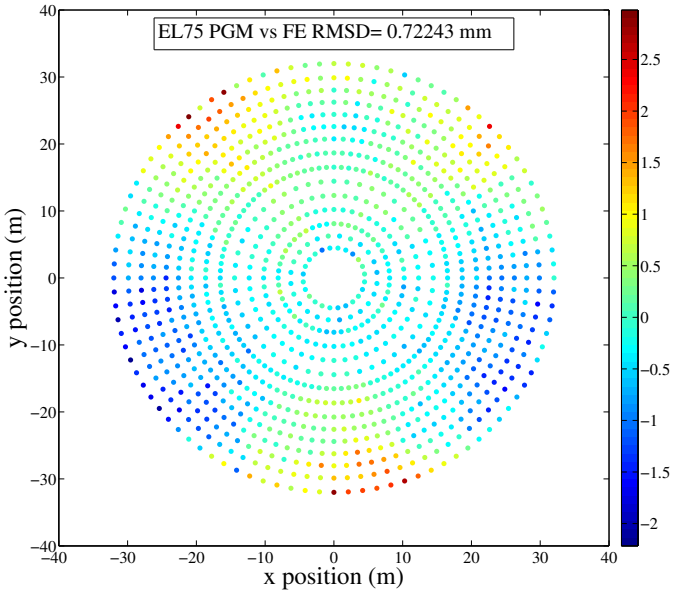

(a) Elevation $\beta = 75°$ without updating

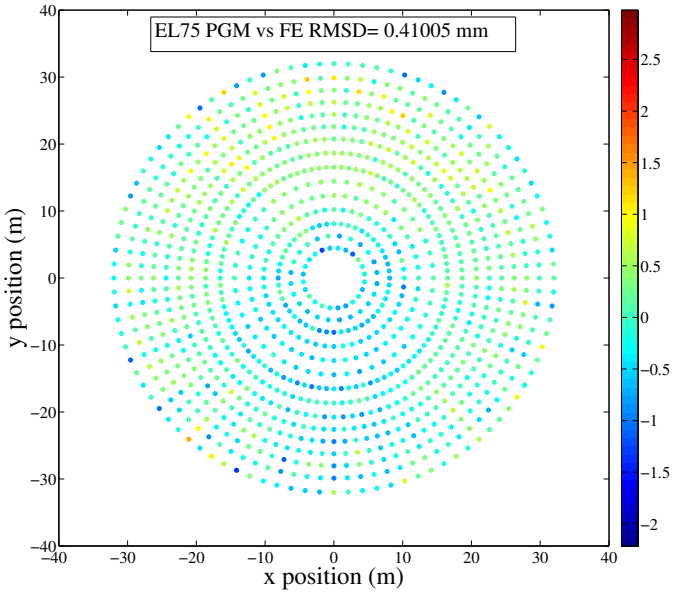

(b) Elevation $\beta = 75°$ with updating

Figure 13. FEM *vs* PGM comparison without (a) and with (b) model updating for elevation angle $\beta = 75°$. Chromatic scale of displacements is in mm.

Please cite this document as: F. Stochino, A. Cazzani, S. Poppi, and E. Turco "Sardinia Radio Telescope Finite Element Model Updating by means of Photogrammetric Measurements" Mathematics and Mechanics of Solids, Vol 22(4), 885–901 DOI:10.1177/1081286515616046

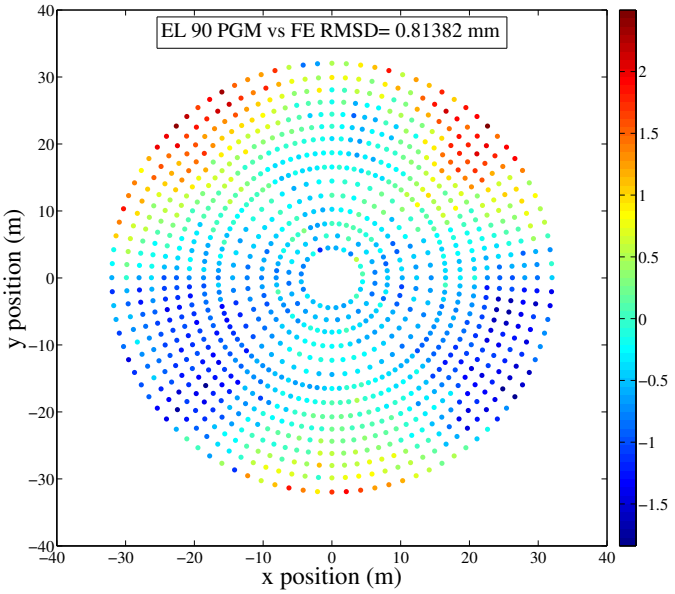

(a) Elevation $\beta = 90°$ without updating

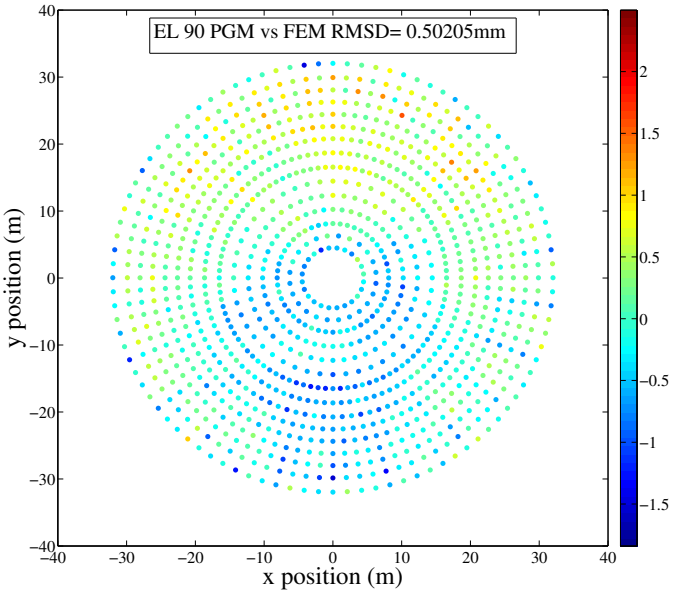

(b) Elevation $\beta = 90°$ with updating

Figure 14. FEM *vs* PGM comparison without (a) and with (b) model updating for elevation angle $\beta = 90°$. Chromatic scale of displacements is in mm.

Please cite this document as: F. Stochino, A. Cazzani, S. Poppi, and E. Turco "Sardinia Radio Telescope Finite Element Model Updating by means of Photogrammetric Measurements" Mathematics and Mechanics of Solids, Vol 22(4), 885–901 DOI:10.1177/1081286515616046

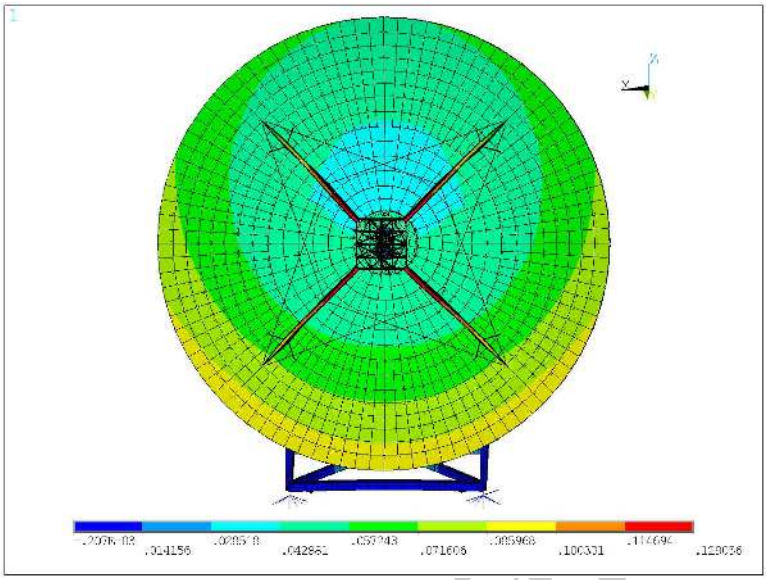

(a) FEM without updating

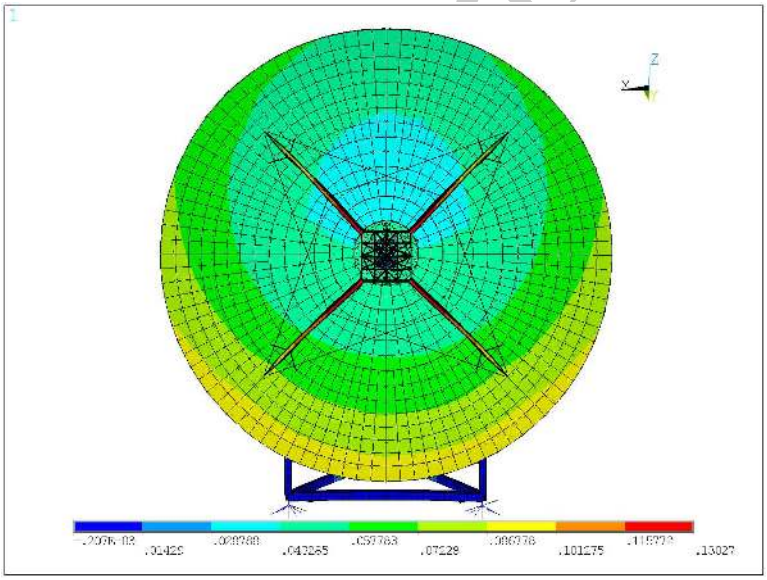

(b) FEM with updating

Figure 15. Vertical displacements (m) by FE model under gravitational load without (a) and with (b) equivalent anelastic strains for elevation angle $\beta = 15°$.

Please cite this document as: F. Stochino, A. Cazzani, S. Poppi, and E. Turco "Sardinia Radio Telescope Finite Element Model Updating by means of Photogrammetric Measurements" Mathematics and Mechanics of Solids, Vol 22(4), 885–901 DOI:10.1177/1081286515616046

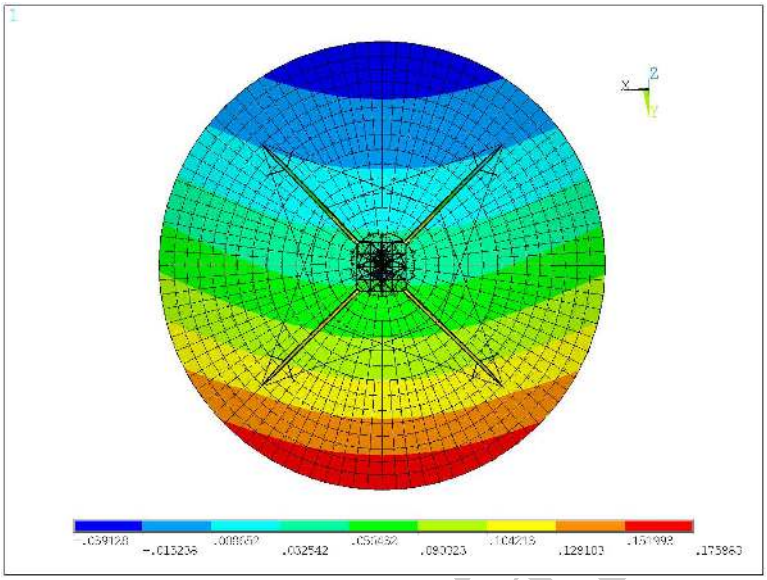

(a) FEM without updating

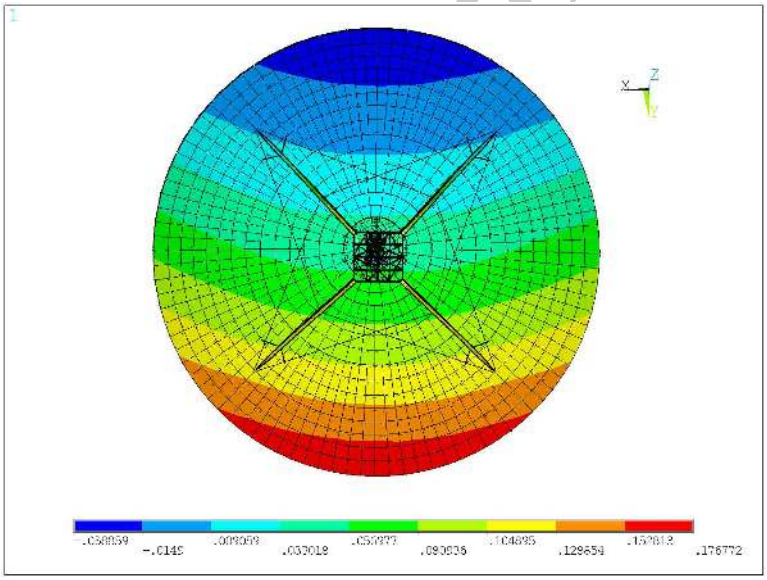

(b) FEM with updating

Figure 16. Vertical displacements (m) by FE model under gravitational load without (a) and with (b) equivalent anelastic strains for elevation angle $\beta = 60°$.

Please cite this document as: F. Stochino, A. Cazzani, S. Poppi, and E. Turco "Sardinia Radio Telescope Finite Element Model Updating by means of Photogrammetric Measurements" Mathematics and Mechanics of Solids, Vol 22(4), 885–901 DOI:10.1177/1081286515616046

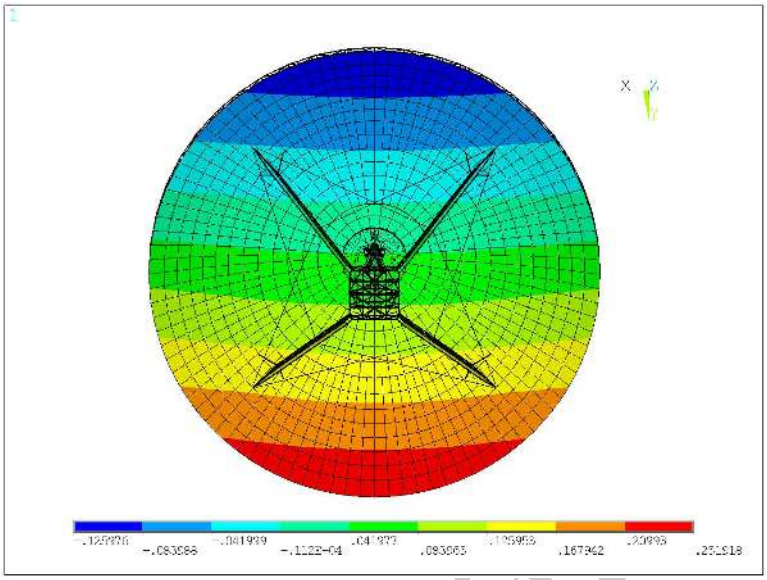

(a) FEM without updating

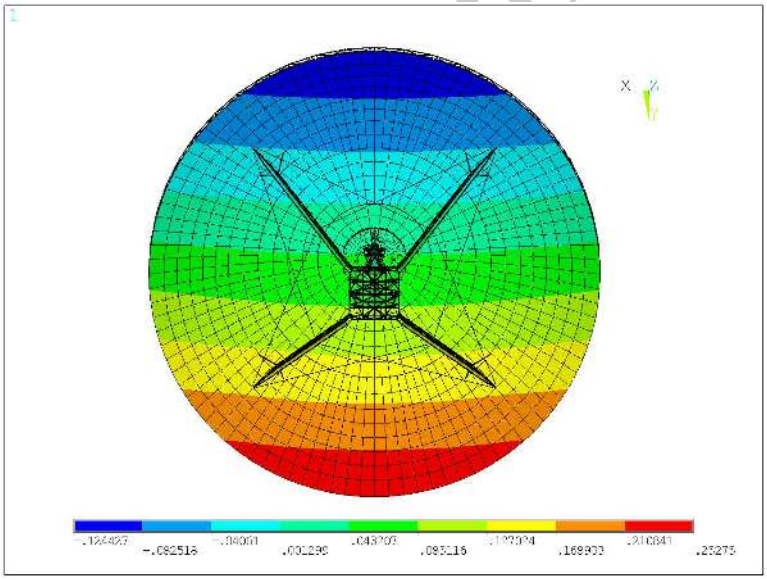

(b) FEM with updating

Figure 17. Vertical displacements (m) by FE model under gravitational load without (a) and with (b) equivalent anelastic strains for elevation angle $\beta = 75°$.

Please cite this document as: F. Stochino, A. Cazzani, S. Poppi, and E. Turco "Sardinia Radio Telescope Finite Element Model Updating by means of Photogrammetric Measurements" Mathematics and Mechanics of Solids, Vol 22(4), 885–901 DOI:10.1177/1081286515616046

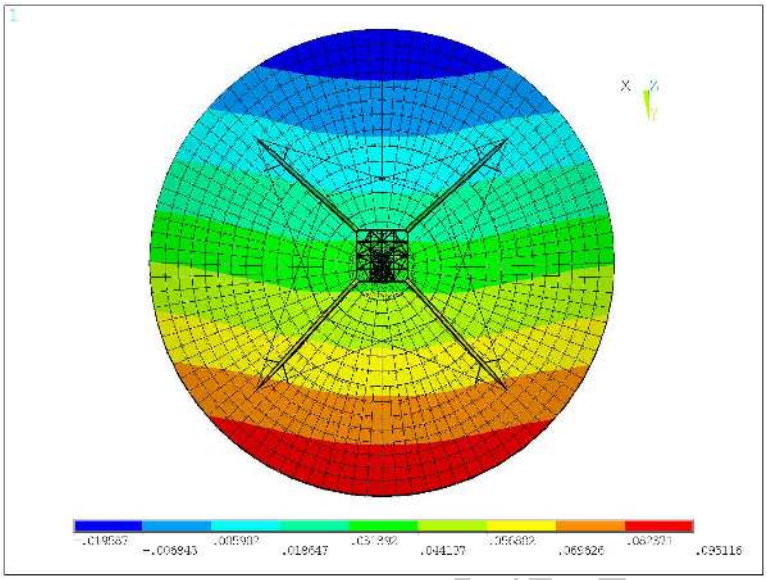

(a) FEM without updating

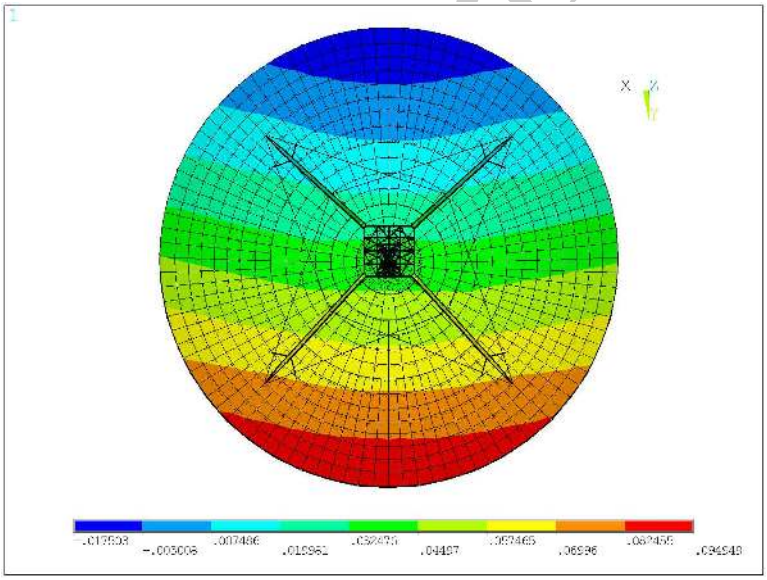

(b) FEM with updating

Figure 18. Vertical displacements (m) by FE model under gravitational load without (a) and with (b) equivalent anelastic strains for elevation angle $\beta = 90°$.

Please cite this document as: F. Stochino, A. Cazzani, S. Poppi, and E. Turco "Sardinia Radio Telescope Finite Element Model Updating by means of Photogrammetric Measurements" Mathematics and Mechanics of Solids, Vol 22(4), 885–901 DOI:10.1177/1081286515616046